

Characterization of a series of sodium molybdate structures by two-dimensional Raman correlation analysis

Boknam Chae,¹ Young Mee Jung,¹ Xianglan Wu² and Seung Bin Kim^{1*}

¹ Department of Chemistry, Laboratory for Vibrational Spectroscopy, Pohang University of Science and Technology, San 31, Hyoja-dong, Pohang 790-784, Republic of Korea

² Power Source Device Team, Electronic and Telecommunications Research Institute, 161 Gajeong-dong, Yuseong-gu, Daejeon 305-350, Republic of Korea

Received 2 January 2003; Accepted 21 April 2003

This paper demonstrates the use of two-dimensional (2D) correlation spectroscopy in the characterization of the sodium molybdate structures that include and are intermediate between the hexagonal and orthorhombic forms; this series of sodium molybdates is produced by varying the preparation conditions, particularly the acid concentration and the heat-treatment temperature. In order to verify the assignments of the vibrational modes of hexagonal sodium molybdate, 2D correlation analysis was applied to the acid concentration-dependent Raman spectra. We can confirm from 2D Raman correlation analysis that this series of preparation conditions results in a series of sodium molybdates including and intermediate between the hexagonal and orthorhombic forms. Furthermore, 2D Raman correlation analysis elucidates the sequence of the structural transformation of hexagonal sodium molybdate into the orthorhombic form. With progression within the series from the hexagonal to the orthorhombic structures, the intensities of the oxygen–molybdenum stretching bands in sodium molybdate change in the following sequence: 973 cm^{-1} (terminal OMo in the hexagonal structure, decrease in intensity) $\rightarrow 996\text{ cm}^{-1}$ (terminal OMo in the orthorhombic structure, increase in intensity) $\rightarrow (897, 881)\text{ cm}^{-1}$ (corner OMo₂ in the hexagonal structure, decrease in intensity) $\rightarrow 664\text{ cm}^{-1}$ (edge OMo₃ in the orthorhombic structure, increase in intensity) $\rightarrow 820\text{ cm}^{-1}$ (corner OMo₂ in the orthorhombic structure, increase in intensity) $\rightarrow 692\text{ cm}^{-1}$ (edge OMo₃ in the hexagonal structure, decrease in intensity). This sequence implies that the changes in the corner OMo₂ and edge OMo₃ structures along the series of sodium molybdates are strongly correlated. Copyright © 2003 John Wiley & Sons, Ltd.

KEYWORDS: hexagonal sodium molybdate; acidification; heat treatment; two-dimensional correlation analysis

INTRODUCTION

Molybdenum oxides with two-dimensional layered structures or three-dimensional tunnel frameworks have drawn much attention as potential cathodic materials for use in secondary lithium batteries.^{1–6} The oxides and oxide hydrates of molybdenum display a variety of structures involving linked MoO₆ octahedra.⁷ There are three well-known structures of molybdenum oxide (MoO₃). The orthorhombic form of MoO₃ is stable and possesses a layered structure of edge-sharing MoO₆ octahedra [Fig. 1(a)].^{8–10} The other

polymorphs of MoO₃ are monoclinic MoO₃ and hexagonal MoO₃. Monoclinic MoO₃ is similar to ReO₃, with its structure of corner-sharing MoO₆ octahedra,¹¹ and the hexagonal MoO₃ framework is constructed of the same zigzag chains of MoO₆ octahedra as found in orthorhombic MoO₃ but they connect through the *cis*-position between the chains [Fig. 1(b)].¹² Moreover, by varying the MoO₃ preparation conditions such as acid type and concentration and the heat-treatment temperature, different forms of MoO₃ can be created.^{13–15}

Sodium molybdates also form different structures under different preparation conditions. The acidification of Na₂MoO₄ solutions with different concentrations of strong acids (e.g. HCl and HNO₃) and the variation of the heat-treatment temperature produce different forms of sodium molybdates.¹⁶ These structural differences influence

*Correspondence to: Seung Bin Kim, Department of Chemistry, Laboratory for Vibrational Spectroscopy, Pohang University of Science and Technology, San 31, Hyoja-dong, Pohang 790-784, Republic of Korea. E-mail: sbkim@postech.edu
Contract/grant sponsor: Korea Research Foundation;
Contract/grant number: BK21.

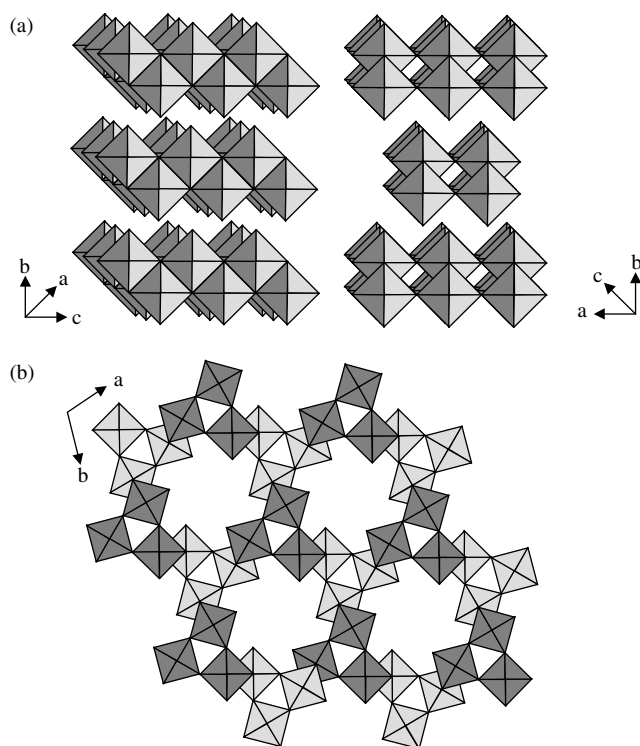


Figure 1. Structures of (a) orthorhombic and (b) hexagonal molybdenum oxides.^{12,15}

the electrochemical behavior, such as the chemical diffusion coefficient of lithium ions in, and the discharge capacity of, secondary lithium batteries.¹⁶

Of the molybdenum oxides, the vibrational spectra of orthorhombic and monoclinic MoO_3 and of various forms of hydrates have previously been analyzed^{17–19} and the Raman- and IR-active modes calculated.²⁰ In addition, polarized Raman and FTIR spectra have been used by Narzri and Julien^{21,22} to study the anisotropic nature of orthorhombic MoO_3 single crystals. Although some vibrational studies of monoclinic MoO_3 have been carried out, the vibrational spectra of hexagonal MoO_3 have not yet been reported. In addition, most of the FTIR spectra of molybdenum oxides have been obtained using the limited KBr disk method.^{23–25} Partial or complete ion exchange, particularly for inorganic salts and for hydrochloride salts of organic amines and other bases, may cause spectral changes that completely preclude any useful purpose for the spectrum.²⁶

In this study, we attempted to assign the vibrational modes of hexagonal sodium molybdate by correlating the structures of the sodium molybdates in the series produced by variation of the heat-treatment temperatures and preparation conditions. Our spectral interpretations are based on the fact that the stretching and bending vibrations of MoO_6 occur in the regions 1000–600 and 400–200 cm^{-1} , respectively. The vibrational modes of the sodium molybdates are classified as those of the terminal MoO bonds, the corner OMO_2 bonds or

the three-coordinated edge OMO_3 oxygen–molybdenum bonds.

In addition, in order to analyze the vibrational modes of oxygen–molybdenum bonds and to describe the structures of the sodium molybdates in the series, we applied two-dimensional (2D) correlation analysis to the acid concentration-dependent Raman spectra. Generalized (2D) correlation spectroscopy has been applied extensively to the analysis of spectral data sets obtained during the observation of a system under some external perturbation.^{27–29} Because of the wide range of applications of this technique, it has become one of the standard analytical techniques for interpreting various types of spectroscopic data. The details of this technique are described elsewhere,^{27–29} so no further description is given here. Through this 2D correlation analysis, we also elucidated the structural correlations between the hexagonal and orthorhombic sodium molybdenum oxides.

EXPERIMENTAL

Materials and preparation

Sodium molybdates were prepared by the acidification of 0.25 M Na_2MoO_4 (Aldrich, 99.99%) solutions with different HCl solutions in the range 1.0–2.5 M as described by Yu *et al.*¹⁶ 100 ml of 0.25 M Na_2MoO_4 solution were added to 100 ml of HCl solutions in the range 1.0–2.5 M. The resulting acidified solutions were heated at 100 °C with constant stirring for 1 h. The resulting solutions were aged for 24 h, then filtered, washed with distilled water, dried at room temperature and heated at 50, 250, 300, 350, or 550 °C for 1 h.

Chemical analysis

Composition analyses of Mo and Na were performed using a Perkin-Elmer inductively coupled plasma mass spectrometer. The water content in the oxides was calculated from the weight loss in the samples using a Perkin-Elmer Pyris 1 TGA thermogravimetric analyzer. TGA analysis was performed in the range 30–600 °C and the heating rate was 10 °C min^{-1} .

Measurements

Powder x-ray diffraction (XRD) measurements were conducted on a Rigaku RINT-2500 vertical diffractometer using $\text{Cu K}\alpha$ radiation. Raman spectra were collected using a Renishaw Raman microscope consisting of an air-cooled charge-coupled device (CCD) detector and an argon ion laser operating at 514.5 nm. 2D correlation analysis was performed using an algorithm based on the numerical method developed by Noda *et al.*²⁸ The 2D correlation analysis was carried out after baseline correction and normalization of the Raman spectra. A subroutine named KG2D³⁰ written in Array Basic language (GRAMS/386; Galactic Industries, Salem, NH, USA) was employed for the 2D correlation analyses.

RESULTS AND DISCUSSION

The series of sodium molybdates

Figure 2 shows the Raman spectra of the sodium molybdates prepared using different dilutions of HCl, resulting in different $\text{Na}^+:\text{H}^+$ ratios (1:2 to 1:5). The series of sodium molybdates in the ratios of $\text{Na}^+:\text{H}^+ = 1:2, 1:3, 1:4$ and $1:5$ had the following chemical compositions: $\text{Na}_{0.15}\text{MoO}_3 \cdot 0.44\text{H}_2\text{O}$, $\text{Na}_{0.16}\text{MoO}_3 \cdot 0.43\text{H}_2\text{O}$, $\text{Na}_{0.070}\text{MoO}_3 \cdot 0.25\text{H}_2\text{O}$ and $\text{Na}_{0.068}\text{MoO}_3 \cdot 0.24\text{H}_2\text{O}$.

The Raman spectrum of $\alpha\text{-MoO}_3$ (the orthorhombic form) is also shown for comparison. The spectral differences are largest between the materials prepared at $\text{Na}^+:\text{H}^+ = 1:2$ and $1:5$; the Raman spectrum of the sodium molybdate prepared at $\text{Na}^+:\text{H}^+ = 1:5$ [Fig. 2(d)] has the same features as that of $\alpha\text{-MoO}_3$ [Fig. 2(e)].

To ascertain the structural differences between these two sodium molybdates, their XRD patterns were obtained (Fig. 3). The XRD pattern of the sodium molybdate prepared at $\text{Na}^+:\text{H}^+ = 1:2$ [Fig. 3(a)] indicates that this sodium molybdate has a hexagonal structure,^{12–16} whereas that of the sodium molybdate prepared at $\text{Na}^+:\text{H}^+ = 1:5$ [Fig. 3(b)] indicates that it has an orthorhombic structure,^{4,12,16,21,22,31} suggesting that as the $\text{Na}^+:\text{H}^+$ ratio used in preparation decreases, the favored structure becomes the orthorhombic form. The XRD pattern of the sodium molybdate prepared at $\text{Na}^+:\text{H}^+ = 1:2$ agreed well with a hexagonal structure as reported by Guo *et al.*¹² and Kumagai *et al.*⁴

On the basis of our information about the structures of the prepared sodium molybdates, we examined their Raman spectra in order to classify their vibrational modes and to follow the variation of structure with varying preparation conditions. It is expected that the Raman spectrum of sodium molybdate prepared at $\text{Na}^+:\text{H}^+ = 1:2$ will indicate a hexagonal structure and that further decrease in the $\text{Na}^+:\text{H}^+$ ratio will produce a partially orthorhombic

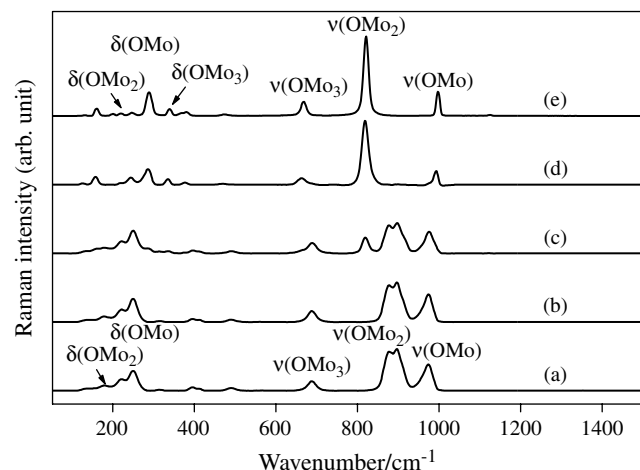


Figure 2. Raman spectra of the sodium molybdates prepared at $\text{Na}^+:\text{H}^+ =$ (a) 1:2, (b) 1:3, (c) 1:4 and (d) 1:5 dried at room temperature. (e) Raman spectrum of $\alpha\text{-MoO}_3$.

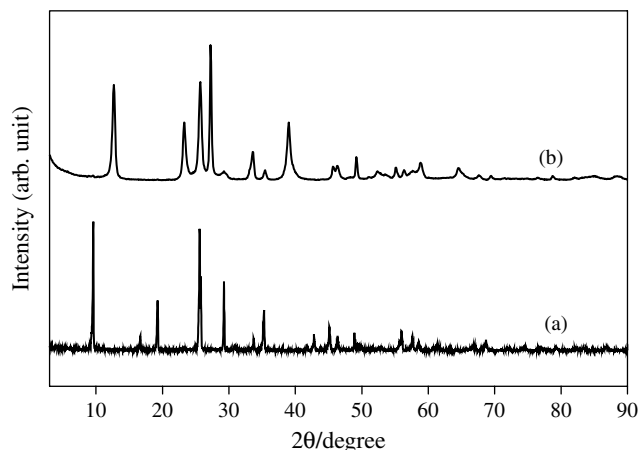


Figure 3. Powder x-ray diffraction patterns of sodium molybdates prepared at $\text{Na}^+:\text{H}^+ =$ (a) 1:2 and (b) 1:5.

phase at $\text{Na}^+:\text{H}^+ = 1:4$; this phase becomes dominant at $\text{Na}^+:\text{H}^+ = 1:5$, as shown in the XRD pattern and reported by Yu *et al.*¹⁶

As shown in Fig. 2(e), bands due to the terminal MoO, the corner OMo_2 and the three-coordinated edge OMo_3 oxygen–molybdenum stretching vibrations of $\alpha\text{-MoO}_3$ appear at 998, 820, and 668 cm^{-1} , respectively.^{17–22} Bands due to the terminal MoO, the corner OMo_2 and to the three-coordinated edge OMo_3 oxygen–molybdenum bending vibrations appear at 289, 219, and 339 cm^{-1} , respectively.^{17–22} For orthorhombic sodium molybdate, the band positions are not very different from those of $\alpha\text{-MoO}_3$; the characteristic Raman bands of hexagonal and orthorhombic sodium molybdate and intermediate forms between them are presented in Table 1. For hexagonal sodium molybdate, bands at 977, 899, 882, 690, 317, 252 and 225 cm^{-1} are observed. From these Raman spectra, it is concluded that the stable phase changes from hexagonal to orthorhombic sodium molybdate; however, it was not possible from these spectra alone to assign the vibrational modes for the molybdenum–oxygen bonds, since the information about the intermediate structures provided by these spectra is not sufficiently detailed.

Therefore, a series of structures including and intermediate between the hexagonal and orthorhombic forms was also produced by variation of the heat treatment temperature. These structural transformations by heat treatment are very similar to that of tungsten oxide. For tungsten oxide, orthorhombic $\text{WO}_3 \cdot \frac{1}{3}\text{H}_2\text{O}$ transformed into hexagonal WO_3 by heat treatment, which was expressed in terms of oriented nucleation of hexagonal oxide on the (001) hydrate plane and of oriented growth. It is therefore suggested that the transformation between hexagonal and orthorhombic forms proceeds through an oriented nucleation and growth mechanism as occurs in the structural transformation of tungsten oxide.^{32,33}

Table 1. Characteristic Raman wavenumbers (cm^{-1}) of $\alpha\text{-MoO}_3$, hexagonal sodium molybdate ($\text{Na}^+:\text{H}^+$ ratio = 1:2) and orthorhombic sodium molybdate ($\text{Na}^+:\text{H}^+$ ratio = 1:5)^a

Structure	$\text{Na}^+:\text{H}^+$				$\alpha\text{-MoO}_3$	Assignment ²¹
	1:2	1:3	1:4	1:5		
Orthorhombic			996	996	996 (996)	$\nu(\text{OMo})$
Hexagonal	977 (973)	977	978			$\nu(\text{OMo})$
Hexagonal	899, 882 (897, 881)	899, 881	899, 880			$\nu(\text{OMo}_2)$
Orthorhombic				821 (820)	821	$\nu(\text{OMo}_2)$
Hexagonal	690 (692)	690	691			$\nu(\text{OMo}_3)$
Orthorhombic			665	666 (664)	668	$\nu(\text{OMo}_3)$
Hexagonal	492	493	492			
Orthorhombic				472	472	
Hexagonal	413, 399	414, 399	414, 399			
Orthorhombic				379	379	
Orthorhombic			337	338 (330)	339	$\delta(\text{OMo}_3)$
Hexagonal	317 (317)	317	317			$\delta(\text{OMo}_3)$
Orthorhombic			289	289 (289)	289	$\delta(\text{OMo})$
Hexagonal	252 (255)	252	252			$\delta(\text{OMo})$
Orthorhombic				246	246	
Hexagonal	225 (222)	225	225			$\delta(\text{OMo}_2)$
Orthorhombic				210, 198	219, 200	$\delta(\text{OMo}_2)$
Hexagonal	183	183	181			
Orthorhombic			161	160	160	
Hexagonal	138	138	137			
Orthorhombic				130	131	

^a Numbers in parentheses are wavenumbers of oxygen–molybdenum modes obtained from the 2D Raman correlation analysis.

Figure 4 shows the Raman spectra of the sodium molybdenum oxides produced at different heat-treatment temperatures. As discussed in the previous section, the structure of sodium molybdate prepared at $\text{Na}^+:\text{H}^+ = 1:2$ is hexagonal and that prepared at $\text{Na}^+:\text{H}^+ = 1:4$ has a mixed hexagonal and orthorhombic structure. With variation of the heat-treatment temperature applied to the sodium molybdate prepared at $\text{Na}^+:\text{H}^+ = 1:4$, a series of structures from the mixed hexagonal form to the stable orthorhombic form was produced. The band at 977 cm^{-1} resolves into two bands at 977 and 996 cm^{-1} with increase in the heat-treatment temperature from 50 to 250°C , and of these only the band at 996 cm^{-1} is observed above 350°C . As the band at 821 cm^{-1} starts to appear with increase in heat-treatment temperature,

the intensities of the bands at 899 and 882 cm^{-1} decrease, and of these only the band at 821 cm^{-1} is observed above 350°C . Further, the band at 690 cm^{-1} also resolves into two bands at 690 and 666 cm^{-1} with increase in heat-treatment temperature, and of these only the band at 666 cm^{-1} is observed above 350°C .

From these results, the vibrational modes of hexagonal sodium molybdate can be assigned as follows because of their correlation with the vibrational modes occurring through the series of structures. The stretching vibrations of the terminal Mo—O bonds appear at 977 cm^{-1} , those of the corner OMo_2 bonds at 899 and 882 cm^{-1} and that of the edge OMo bonds at 690 cm^{-1} . In a similar manner, we can also assign the bending vibrational modes of the molybdenum oxides. The

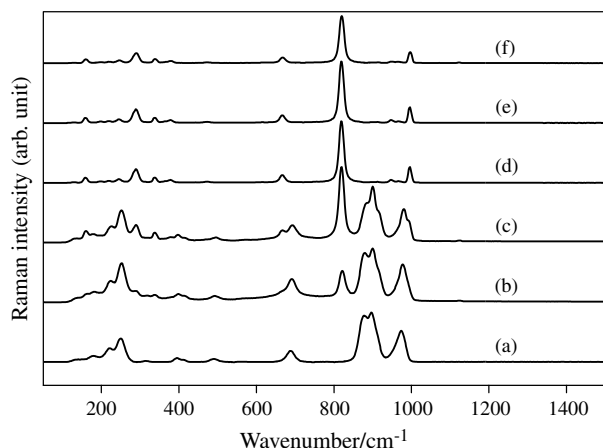


Figure 4. Raman spectra of sodium molybdates prepared at (a) $\text{Na}^+:\text{H}^+ = 1:2$ and $\text{Na}^+:\text{H}^+ = 1:4$ heat-treated at (b) 50, (c) 250, (d) 300, (e) 350 and (f) 550 °C.

bending vibrations of edge OMo_3 appear at 317 cm^{-1} , those of terminal OMo at 252 cm^{-1} and those of corner OMo_2 at 225 cm^{-1} . Table 2 shows the characteristic Raman bands of hexagonal and orthorhombic sodium molybdate, and intermediates between them for the various heat-treatment temperatures.

Comparing the Raman spectra of the hexagonal and orthorhombic sodium molybdates, it is found that the terminal $\nu(\text{OMo})$ mode in the hexagonal structure is shifted to lower wavenumber by about 20 cm^{-1} , whereas the corner $\nu(\text{OMo}_2)$ and edge $\nu(\text{OMo}_3)$ modes in the hexagonal structure are shifted to higher wavenumbers by about 80

and 25 cm^{-1} , respectively. This suggests that the change in structure is strongly correlated with the band shifts of vibrational modes of hexagonal sodium molybdate. This large up-shift (80 cm^{-1}) is not understandable in terms of the bond strength, although the wavenumber down-shift of the terminal $\text{Mo}=\text{O}$ bond can be explained that the strength of the $\text{Mo}=\text{O}$ double bond in the hexagonal form is weakened due to the ionic interaction between the terminal oxygen and sodium ion with water together in the tunnel as described by Guo *et al.*¹² Hence other effects should possibly be considered. The links between the zigzag chains in hexagonal sodium molybdates occur through adjacent (*cis*) oxygens rather than through opposing (*trans*) oxygens, as in the orthorhombic structure.^{15,34} This difference may cause both bond strength and bond angle changes, which could influence the wavenumbers of the vibrational modes of the $\text{Mo}=\text{O}$ bonds, as suggested for $\text{Si}=\text{O}$ bonds in oxide glasses by Sharma *et al.*³⁵ At various pressures, the bond angle changes of the $\text{Si}-\text{O}-\text{Si}$ linkage in K_2SiO_9 glass influence the wavenumber of the vibrational mode of the $\text{Si}-\text{O}-\text{Si}$ bond.

2D Raman correlation analysis

To investigate further the structural differences in the series from hexagonal to orthorhombic sodium molybdate, we applied 2D correlation analysis to the acid concentration-dependent Raman spectra. 2D Raman correlation spectra were constructed from the Raman spectra of the sodium molybdate prepared at $\text{Na}^+:\text{H}^+ = 1:2, 1:3, 1:4$, and $1:5$ as shown in Fig. 2. We focused on the spectral region $1100\text{--}100\text{ cm}^{-1}$. This range provides information about the

Table 2. Characteristic Raman wavenumbers (cm^{-1}) of hexagonal sodium molybdate ($\text{Na}^+:\text{H}^+$ ratio = $1:2$ and 25°C) and orthorhombic sodium molybdate ($\text{Na}^+:\text{H}^+$ ratio = $1:4$ and 550°C)

Structure	Na ⁺ :H ⁺						Assignment ²¹
	1:2	1:4					
	25 °C	50 °C	250 °C	300 °C	350 °C	550 °C	
Orthorhombic				996	996	996	ν(OMo)
Hexagonal	977	978	978				ν(OMo)
Hexagonal	899, 882	899, 880	891, 882				ν(OMo ₂)
Orthorhombic		821	821	821	821	821	ν(OMo ₂)
Hexagonal	690	691	692				ν(OMo ₃)
Orthorhombic		665	666	666	666	666	ν(OMo ₃)
Hexagonal	492	492	492				
Orthorhombic				472	472	472	
Orthorhombic		337	338	338	338	338	δ(OMo ₃)
Hexagonal	317	317					δ(OMo ₃)
Orthorhombic		289	289	289	289	289	δ(OMo)
Hexagonal	252	252	252				δ(OMo)
Orthorhombic				245	245	245	
Hexagonal	225	225	227				δ(OMo ₂)
Orthorhombic				219	219	219	δ(OMo ₂)

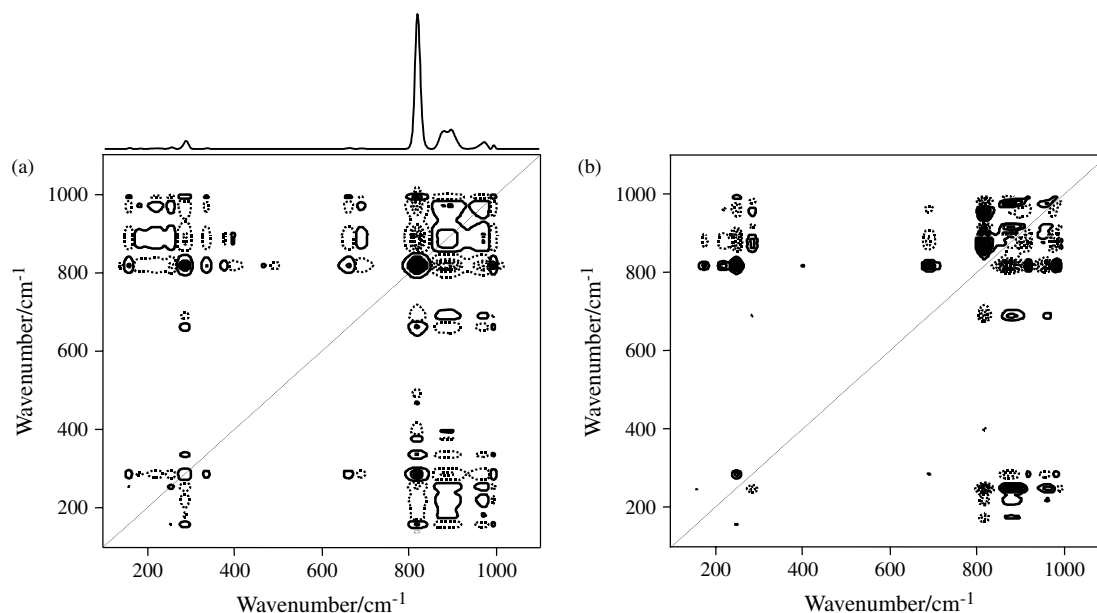


Figure 5. (a) Synchronous and (b) asynchronous 2D Raman correlation spectra generated from the acid concentration-dependent spectra of the sodium molybdates in the spectral region $1100\text{--}100\text{ cm}^{-1}$. Solid and dotted lines represent positive and negative cross peaks, respectively.

oxygen–molybdenum stretching and bending vibrations. The synchronous and asynchronous 2D Raman correlation spectra are displayed in Fig. 5(a) and (b), respectively. A power spectrum is also shown at the top of Fig. 5(a). The power spectrum in Fig. 5(a) yields bands at 996, 973, 897, 881, 820, 692, 664, 339, 317, 289, and 255 cm^{-1} . The band at 820 cm^{-1} (assigned to the stretching vibration of corner MoO_2 in orthorhombic sodium molybdate) shows much greater intensity variation in the series of spectra than other bands; the bands at 897 and 881 cm^{-1} (assigned to the stretching vibrations of corner MoO_2 in hexagonal sodium molybdate) also show some intensity variation, suggesting that corner Mo—O—Mo bonds are strongly influenced by the variation of structure produced by the different $\text{Na}^+:\text{H}^+$ preparation ratios. Table 1 summarizes the wavenumbers of oxygen–molybdenum modes of hexagonal and orthorhombic sodium molybdate and intermediate forms between them with wavenumbers obtained from the 2D Raman correlation analysis.

In the synchronous 2D correlation spectrum, the presence of positive cross peaks at $(996, 820)$, $(996, 664)$, $(996, 339)$ and $(996, 289)\text{ cm}^{-1}$ reveals that these vibrational modes, which increase in intensity with increasing $\text{Na}^+:\text{H}^+$ ratio, originate from orthorhombic sodium molybdate, while the presence of positive cross peaks observed at $(973, 897)$, $(973, 881)$, $(973, 692)$, $(973, 255)$ and $(973, 222)\text{ cm}^{-1}$ suggest that these vibrational modes which decrease in intensity with increasing $\text{Na}^+:\text{H}^+$ ratio originate from hexagonal sodium molybdate. In addition, the negative cross peaks at $(222, 820)$, $(255, 820)$, $(692, 820)$, $(881, 820)$, $(897, 820)$ and $(973, 820)\text{ cm}^{-1}$ reveal that with increases in the $\text{Na}^+:\text{H}^+$ ratio the intensity

of the band at 820 cm^{-1} (assigned to orthorhombic sodium molybdate) increases, whereas bands at 973, 897, 881, 692, 255 and 222 cm^{-1} (assigned to hexagonal sodium molybdate) decrease in intensity. Other negative cross peaks at $(881, 664)$ and $(897, 664)\text{ cm}^{-1}$ also reveal that with increases in the $\text{Na}^+:\text{H}^+$ ratio the intensity of the band at 664 cm^{-1} (assigned to orthorhombic sodium molybdate) increases while the bands at 881 and 897 cm^{-1} (assigned to hexagonal sodium molybdate) decrease in intensity. Additional information is then provided by the asynchronous spectrum, from which it is possible to determine the sequence of spectral changes as the $\text{Na}^+:\text{H}^+$ ratio increases.

The synchronous and asynchronous 2D Raman correlation spectra for the region $1100\text{--}600\text{ cm}^{-1}$ are displayed in Fig. 6, providing more detailed information about the progression of structural differences within the series. The power spectrum extracted along the diagonal line of the synchronous spectrum is shown at the top of Fig. 6(a). The positive cross peaks at $(664, 820)$ and $(996, 820)\text{ cm}^{-1}$ in the synchronous 2D correlation spectrum [Fig. 5(a)] show that the intensities of those bands increase with increases in acid concentration. This result confirms that the sequence of structures of sodium molybdates prepared with increasing $\text{Na}^+:\text{H}^+$ ratios is from a hexagonal to an orthorhombic structure.

According to the rule proposed by Noda,²⁷ the signs of the cross peaks in the asynchronous 2D correlation spectrum [Fig. 6(b)] imply the following sequence of spectral changes in the bands assigned to hexagonal sodium molybdate as the $\text{Na}^+:\text{H}^+$ ratio increases: $973\text{ cm}^{-1} \rightarrow (897, 881)\text{ cm}^{-1} \rightarrow 692\text{ cm}^{-1}$, i.e. the intensity of the band due to terminal

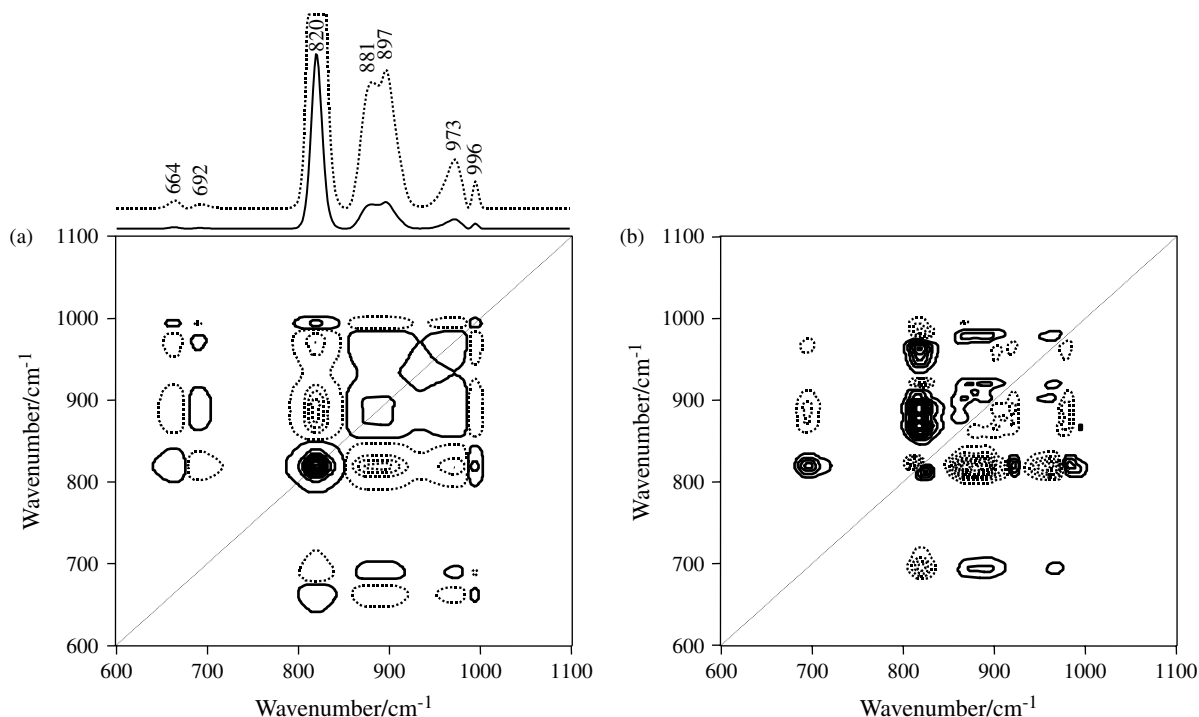


Figure 6. (a) Synchronous and (b) asynchronous 2D Raman correlation spectra generated from acid concentration-dependent spectra of the sodium molybdates in the spectral region 1100–600 cm^{-1} . Solid and dotted lines represent positive and negative cross peaks, respectively.

OMo changes first, then the intensity of the band due to corner OMo₂ decreases and then the intensity of the band due to edge OMo₃ decreases. For the bands assigned to orthorhombic sodium molybdate, the spectral changes occur in the following sequence: 996 \rightarrow 664 \rightarrow 820 cm^{-1} , i.e. the intensity of the band due to terminal OMo changes first, then the intensity of the band due to edge OMo₃ increases and then the intensity of the band due to corner OMo₂ increases. Collectively, the spectral changes of the bands assigned to hexagonal sodium molybdate occur in the following sequence: 973 \rightarrow 996 \rightarrow (897, 881) \rightarrow 664 \rightarrow 820 \rightarrow 692 cm^{-1} . As the Na⁺:H⁺ ratio increases, the intensity of the stretching band correlated with terminal OMo in hexagonal sodium molybdate (the intensity of the stretching band due to hexagonal sodium molybdate decreases before the intensity of the stretching band in orthorhombic sodium molybdate increases) changes first, then that correlated with corner OMo₂ in hexagonal sodium molybdate decrease in intensity, that correlated with edge OMo₃ in orthorhombic sodium molybdate increases in intensity, those correlated with corner OMo₂ in orthorhombic sodium molybdate increases in intensity and then that due to the edge OMo₃ in hexagonal sodium molybdate decreases in intensity. These results imply that the changes in the corner OMo₂ and edge OMo₂ structures along the series of sodium molybdates are strongly correlated. In addition, the intensities of the bending modes of oxygen–molybdenum in sodium molybdate also

change according to the sequence of the stretching bands of oxygen–molybdenum.

CONCLUSION

We analyzed the correlation of the structures in a series including and intermediate between hexagonal and orthorhombic sodium molybdate by 2D Raman correlation analysis. The 2D Raman correlation analysis revealed that with increase in the Na⁺:H⁺ ratio the bands at 996, 820 and 664 cm^{-1} (assigned to orthorhombic sodium molybdate) increase in intensity, while the bands at 973, 897, 881 and 692 cm^{-1} (assigned to hexagonal sodium molybdate) decrease in intensity. This result confirms that the series of sodium molybdates moves from hexagonal to orthorhombic structures with increasing Na⁺:H⁺ ratio. The sequence of spectral changes as the acid concentration increases is as follows: 973 cm^{-1} (terminal OMo in hexagonal) \rightarrow 996 cm^{-1} (terminal OMo in orthorhombic) \rightarrow (897, 881) cm^{-1} (corner OMo₂ in hexagonal) \rightarrow 664 cm^{-1} (edge OMo₃ in orthorhombic) \rightarrow 820 cm^{-1} (corner OMo₂ in orthorhombic MoO₃) \rightarrow 692 cm^{-1} (edge OMo₃ in hexagonal). These results imply that there is a strong correlation between the changes in the corner and edge structures within the series of sodium molybdates.

Acknowledgments

This study was supported by the Korea Research Foundation (BK21 Project).

REFERENCES

1. Tsumura T, Inagaki M. *Solid State Ionics* 1997; **104**: 183.
2. Chrustian PA, Carides JN, Disalvo FJ, Waszczak JV. *J. Electrochem. Soc.* 1980; **127**: 2315.
3. Cignini P, Lcovi M, Panero S, Pistoia G, Temperoni C. *J. Electroanal. Chem.* 1979; **102**: 333.
4. Kumagai N, Kumagai N, Tanno K. *Electrochim. Acta* 1987; **32**: 1521.
5. Manthiram A, Tsang CJ. *J. Electrochem. Soc.* 1996; **143**: L143.
6. Guzman G, Yebka B, Livage J, Julien C. *Solid State Ionics* 1996; **86–88**: 407.
7. Braithwait ER, Haber J. *J. Molybdenum: an Outline of Its Chemistry and Uses*. Elsevier: Amsterdam, 1994; chapt. 3.
8. Cora F, Patel A, Harrison N, Roetti MC, Catlow CR. *J. Mater. Chem.* 1997; **7**: 959.
9. Crouch-Baker S, Dickens PG. *Solid State Ionics* 1989; **32–33**: 219.
10. McCarron EM III. *J. Chem. Soc. Chem. Commun.* 1986; **336**.
11. Parise JB, McCarron EM III. *J. Solid State Chem.* 1991; **93**: 193.
12. Guo J, Zavalij P, Whittingham MS. *J. Solid State Chem.* 1995; **117**: 323.
13. Gaiger NA, Baker SC, Dickens PG, James GS. *J. Solid State. Chem.* 1987; **67**: 369.
14. Hu Y, Davis PK, Feist TP. *Solid State Ionics* 1992; **53–56**: 539.
15. McCarron EM III, Thomas DM, Calabrese JC. *Inorg. Chem.* 1987; **26**: 370.
16. Yu A, Kumagai N, Liu Z, Lee JY. *Solid State Ionics* 1998; **11–18**: 11.
17. Seguin L, Figlarz M, Cavagnat R, Lassegues J-C. *Spectrochim. Acta, Part A* 1995; **51**: 1323.
18. Eda K, Sotani N. *Bull. Chem. Soc. Jpn.* 1989; **62**: 4039.
19. Du X, Dong L, Li C, Liang Y, Chen Y. *Langmuir* 1999; **15**: 1693.
20. Py MA, Maschke K. *Physica B* 1981; **105**: 370.
21. Narzri GA, Julien C. *Solid State Ionics* 1992; **53–56**: 376.
22. Julien C, Narzri GA. *Solid State Ionics* 1994; **68**: 111.
23. Ohno T, Miyata H, Hatayama F, Sotani N. *Bull. Chem. Soc. Jpn.* 1987; **60**: 3435.
24. Eda K. *J. Mater. Chem.* 1992; **2**: 533.
25. Sotani N, Kawamoto Y, Inui M. *Mater. Res. Bull.* 1983; **18**: 797.
26. Smith AL. *Applied Infrared Spectroscopy*. Wiley-Interscience: New York, 1979; 83.
27. Noda I. *Appl. Spectrosc.* 1993; **47**: 1329.
28. Noda I, Dowrey AE, Marcott C, Story GM. *Appl. Spectrosc.* 2000; **54**: 236A.
29. Noda I. *Appl. Spectrosc.* 2000; **54**: 994.
30. Ozaki Y. <http://science.kwansei.ac.jp/~ozaki/>.
31. Komaba S, Kumagai N, Kumagai R, Kumagai N, Yashiro H. *Solid State Ionics* 2002; **152–153**: 319.
32. Harb R, Gerand B, Nowogrocki G, Figlarz M. *Solid State Ionics* 1989; **32–33**: 84.
33. Figlarz M. *Prog. Solid State Chem.* 1989; **19**: 1.
34. Kihlborg L. *Ark. Kem.* 1963; **21**: 357.
35. Sharma K, Wang Z, van der Lann S. *J. Raman Spectrosc.* 1996; **27**: 739.